Structural Durability & Health Monitoring

Tech Science Press

https://doi.org/10.32604/sdhm.2026.081608

ARTICLE

A Case Study of the Coupling Mechanism between Urban Site Conditions and High-Rise Building Response Revealed by Ambient Vibration Observations

Yangkai Ou and Boi-Yee Liao*

Department of Engineering, International College, Krirk University, Bangkok, Thailand

*Corresponding Author: Boi-Yee Liao. Email: y5708211@ms18.hinet.net

Received: 05 March 2026; Accepted: 11 May 2026; Published: 24 August 2026

ABSTRACT: Based on three-component (E–N–Z) ambient vibration observations, this study investigates the dynamic characteristics of shallow subsurface conditions and their influence on the seismic response of a high-rise building in a complex urban environment. Ambient vibration measurements were conducted to characterize site dynamic properties and to explore their relationship with structural vibration behavior. Frequency, amplification factor, and site vulnerability index were extracted using the horizontal-to-vertical (H/V) spectral ratio method applied to ambient vibration records. An empirical relationship between the fundamental frequency and sedimentary layer thickness was established using ambient vibration observations and borehole investigation data, and the least-squares method was further applied to invert the spatial distribution of sediment thickness across the study area. The inversion results show good agreement with borehole measurements and exhibit relatively small errors, demonstrating the reliability of the proposed approach for estimating shallow subsurface structures under heterogeneous site conditions. Floor response spectra were further introduced to analyze the variation of structural seismic response along the building height, enabling an integrated interpretation of the coupling between shallow site conditions and floor-level vibration amplification. The results indicate that horizontal vibration amplification is most pronounced near the characteristic period of the design response spectrum, whereas vertical amplification is generally weaker and exhibits a more complex distribution pattern. This study reveals a frequency-mismatch-controlled site–structure interaction mechanism and proposes an integrated observational framework combining ambient vibration analysis and structural response characterization, providing new insights into seismic response assessment of high-rise buildings.

KEYWORDS: Ambient vibration; H/V; floor response spectra; fundamental frequency; site–structure interaction; high-rise building

1 Introduction

The rapid acceleration of urbanization has led to the extensive construction of high-rise buildings in densely developed and geologically complex urban environments, which has attracted increasing attention to their dynamic responses under seismic loading and ambient environmental vibrations. Post earthquake damage surveys and seismic hazard investigations consistently show that even buildings designed with the same fortification intensity, structural system, and material properties may experience markedly different damage levels due to variations in local site conditions. In particular, the geometry, stratification, and mechanical properties of shallow subsurface media play a decisive role in modifying the amplitude, frequency content, and duration of ground motion, thereby directly influencing the seismic input transmitted to superstructures. These site dependent effects may further interact with the inherent dynamic characteristics of high-rise buildings, giving rise to complex site structure interaction phenomena. A systematic and quantitative investigation of the influence of shallow site conditions on the dynamic response of high-rise buildings is therefore essential for improving urban seismic risk assessment, advancing performance based seismic design strategies, and enhancing the resilience of rapidly developing cities [1–4].

Traditional site dynamic characterization primarily relies on drilling surveys, *in situ* testing, and artificial excitation methods, which provide reliable parameters for subsurface structural conditions. However, implementing large scale and high density investigations in densely developed urban areas remains challenging because of construction limitations, high costs, and restricted available space [5,6]. In contrast, passive source detection methods that utilize environmental microtremor offer advantages such as non-destructiveness, low cost, and flexible deployment. These methods have gained popularity in urban site condition assessment and engineering seismic research in recent years [7,8]. Among these techniques, the H/V spectral ratio method is widely employed to characterize the dynamic properties of shallow sedimentary structures. This method analyzes the spectral characteristics of various components in the microtremor record, effectively identifying the site's main frequency and amplification effects. Research indicates that the primary peak frequency of the H/V curve is often closely associated with the fundamental frequency of the sedimentary layer. This relationship can be utilized, in conjunction with quarter-wavelength theory or empirical relationships, to invert the thickness of the sedimentary layer and the shear wave velocity [9–11].

In high-rise buildings, ground or environmental vibrations transmitted through the foundation experience complex processes of propagation, amplification, and attenuation as they travel within the structural system. The transmission of vibration between floors is governed not only by the intrinsic dynamic properties of the building but also by the spectral characteristics of the input motion originating from the site. When the fundamental or lower order vibration frequencies of the structure coincide with or approach the fundamental frequency of the site, significant resonance amplification may occur. This frequency coupling represents a typical manifestation of site structure interaction. Therefore, integrating the analysis of site dynamic behavior with the internal vibration transmission characteristics of buildings is essential for achieving a comprehensive understanding of the dynamic response of high rise structures [12–15].

Previous studies have extensively investigated site effects using ambient vibration methods, particularly through the H/V spectral ratio technique, which has been widely applied for estimating fundamental frequency and sediment thickness. Meanwhile, the dynamic characteristics of high-rise buildings have been analyzed using response spectra and modal analysis methods. In addition, site–structure interaction has been studied through analytical and numerical approaches, highlighting the importance of frequency relationships between site conditions and structural response [16,17]. However, most existing studies focus either on site characterization or on structural response independently, and relatively few studies integrate ambient vibration–based site analysis with *in-situ* structural response observations to investigate their coupling mechanism in real urban environments.

Therefore, this study aims to bridge the gap between site characterization and structural response analysis by proposing an integrated observational framework. The main contributions of this study can be summarized as follows:

(1) A coupled observational framework integrating ambient vibration–based site characterization with structural response analysis is established.
(2) A quantitative relationship between sediment thickness and fundamental frequency is developed using combined ambient vibration data and borehole constraints.
(3) A frequency-mismatch-controlled interaction mechanism is identified, demonstrating that structural response is governed by site-induced spectral modulation and structural modal filtering rather than classical resonance.

2 Theoretical Methods and Data Collection

2.1 Theoretical Methods

The H/V spectral ratio method operates on the principle that various components of the microtremor record exhibit distinct responses to shallow sedimentary structures. Urban microseismic signals generally consist of multiple weak seismic sources, including distant earthquakes, traffic, wind-induced vibrations, and industrial activities, all of which contribute stable energy input. During propagation, the vertical component is predominantly influenced by body waves, which are minimally affected by the overburden layer. In contrast, the horizontal component is more susceptible to variations in impedance, interface reflections, and multiple scattering. Consequently, horizontal energy may experience significant amplification within a specific frequency band, resulting in a prominent peak in the H/V curve when the frequency of the incident wave aligns with the standing wave condition of the shear wave [18].

Site master frequency and amplification factor extraction. A Hanning window was applied to the E–N–Z microtremor recordings and a fast Fourier transform (FFT) was computed [19]:

$$\frac{H}{V}(f) = \frac{\sqrt{H_{NS}^2(f) + H_{EW}^2(f)}}{V_Z(f)}, \tag{1}$$

where $H_{NS}^2(f)$, $H_{EW}^2(f)$, and $V_z(f)$ are the amplitude spectra in the north-south, east-west and vertical directions, respectively. The most prominent peaks of the H/V curves arise from the standing wave effect of the sedimentary layers. The peak frequencies are defined as the primary resonance frequency at the site, with the peak amplitude serving as the amplification coefficient. This coefficient reflects the vibration amplification capacity of the sedimentary layers within this frequency band [20].

The prominent peaks observed in the H/V spectral ratio curves are generally associated with the f_0 of the site, reflecting the dominant dynamic behavior of the shallow sedimentary structure. This fundamental frequency can be further transformed into an eigenperiod, which serves as a representative parameter characterizing the overall dynamic properties of the sedimentary layer. In microtremor analysis, the principal site frequency identified from the H/V spectral ratio is commonly converted into a corresponding characteristic period for subsequent interpretation and comparison with engineering design parameters [21]:

$$T_0 = \frac{1}{f_0}, \tag{2}$$

where f_0 is the fundamental frequency of the site.

Quarter-wavelength theory in relation to f_0 and sediment thickness. The classical quarter-wavelength theory states that f_0 of the sedimentary layer for SH waves is given by [22]:

$$f_0 = \frac{V_s}{4h}, \tag{3}$$

V_s is the average shear-wave velocity of the sedimentary layer, and h represents its thickness. This theoretical relationship provides the basis for inverting the dynamic parameters of sedimentary layers using microtremor data. It is commonly applied to estimate the site fundamental frequency and to investigate shallow subsurface velocity structures. Moreover, the relationship between the predominant period and sediment thickness can be compared with the dynamic characteristics of building structures.

There is usually a power function relationship between the depth of the soil-rock interface and the peak frequency of the H/V spectral ratio curve [23]:

$$h = af_0^b; \ln h = \ln a + b \ln f_0, \tag{4}$$

where a and b are empirical constants related to subsurface conditions. The parameters were estimated using the least squares method based on the linear regression between $\ln f_0$ and $\ln h$, constrained by ambient vibration measurements and borehole data [24].

The site susceptibility value K index proposed by Nakamura was further used to synthesize and describe the resonance and amplification effects of the site [25]:

$$K = \frac{A_0}{f_0}, \tag{5}$$

where A_0 is the peak amplitude of the H/V spectral ratio.

The floor response spectrum (FRS) characterizes the relative amplification of structural dynamic response at different floors under seismic excitation. In this study, a linear single-degree-of-freedom (SDOF) oscillator model is employed to calculate the acceleration response spectra for each floor, assuming a constant structural damping ratio of 5% throughout the analysis, which is commonly adopted for reinforced concrete structures under elastic conditions. The horizontal acceleration response spectrum is obtained by synthesizing the response spectra of two orthogonal horizontal components in the east–west and north–south directions. Accordingly, the horizontal floor response spectral ratio between two floors is defined as:

$$FRS_{i/j}^{H}(T) = \frac{\sqrt{\left[S_{a,E}^{i}(T)\right]^2 + \left[S_{a,N}^{i}(T)\right]^2}}{\sqrt{\left[S_{a,E}^{j}(T)\right]^2 + \left[S_{a,N}^{j}(T)\right]^2}}, \tag{6}$$

where $S_{a,E}(T)$ and $S_{a,N}(T)$ represent the acceleration response spectra derived from the east–west and north–south acceleration time series, respectively, and T denotes the vibration period of the single-degree-of-freedom system. $FRS_{i/j}^{H}(T)$ denotes the horizontal floor response spectral ratio of floor i relative to floor j, and the superscript H indicates the horizontal component.

The vertical direction floor response spectrum ratio is then defined based on the vertical acceleration response spectrum:

$$FRS_{i/j}^{V}(T) = \frac{S_{a,Z}^{i}(T)}{S_{a,Z}^{j}(T)}, \tag{7}$$

where $S_{a,Z}^{i}(T)$ and $S_{a,Z}^{j}(T)$ represent the vertical acceleration response spectra of floors i and j, respectively [26].

2.2 Data Collection

According to the specific conditions of the study area, a total of 101 microtremor observation points were deployed, as shown in Fig. 1. In this study, a E–N–Z broadband intelligent geophone (IGU-BD3C-5) was used in combination with the H/V spectral ratio method to conduct ambient vibration measurements. The observation points were distributed to ensure adequate spatial coverage of the study area, with denser measurements arranged around the building and relatively uniform distribution in the surrounding free-field area. Each measurement lasted approximately 20–30 min to ensure stable recording of ambient vibrations. During data acquisition, environmental disturbances were minimized as much as possible, and data quality was controlled through real-time monitoring and subsequent screening to remove abnormal records.

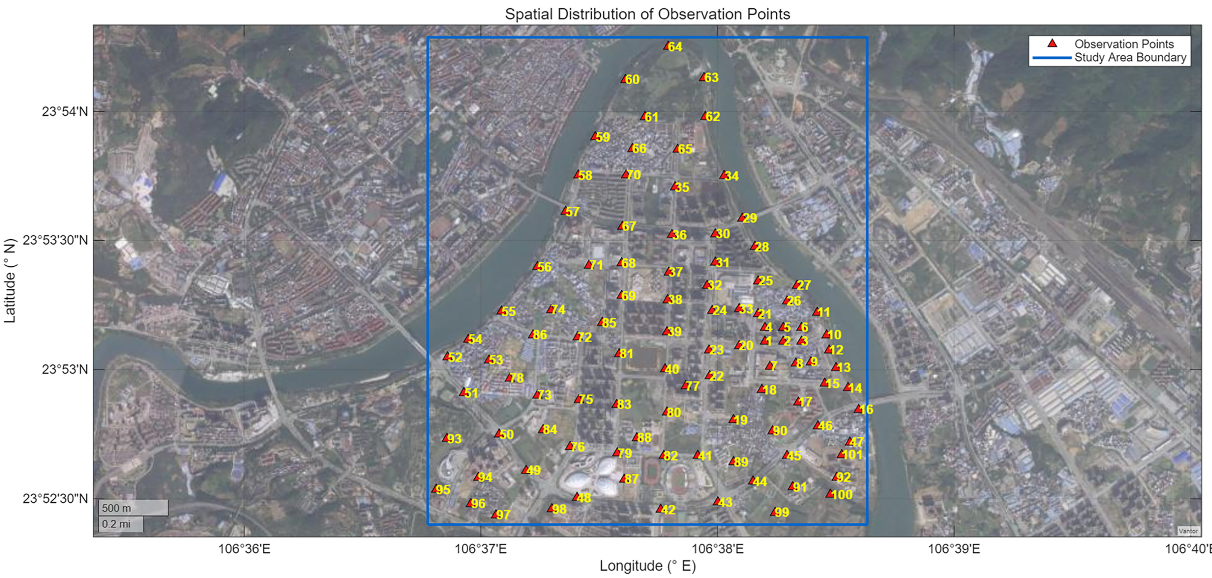

Figure 1: Specific distribution of the study area and observation sites.

Among them, three points are arranged inside the building at the bottom, middle, and top floors to capture the variation of vibration response characteristics along the building height. In the adjacent free field area, observation points are deployed with high density to obtain high resolution micro motion information. The remaining points are distributed relatively uniformly across the study area to characterize the spatial variability of site conditions using the H over V spectral ratio method. All observation points are recorded with a sampling interval of 0.25 ms, corresponding to a sampling frequency of 4000 Hz. This relatively high sampling rate was adopted to ensure high temporal resolution and to accurately capture potential transient components in the ambient vibration signals. Although the primary frequency band of interest in this study is within 0.1–20 Hz, the high sampling frequency helps prevent aliasing effects and improves the stability of spectral estimation. In subsequent processing, band-pass filtering was applied to restrict the effective frequency range to the target band relevant for site response analysis. In addition, positioning and time synchronization are achieved using the Global Navigation Satellite System (GNSS) based on the Global Positioning System (GPS) during data acquisition.

The collected raw microtremor signals underwent processing that included abnormal data rejection and time period segmentation. Subsequently, padpow2-based zero complement, band-pass filtering, FFT spectrum calculation, energy normalization, and smoothing were performed. The instrument's upper and lower impedance limits are 2035 and 1665 Ω, respectively. The natural frequency range spans from 0.16 to 0.24 Hz, with a sensitivity of 160 to 240 Vs/m. The channel gain is uniformly set at 6 dB, ensuring the consistency of the amplitude across the three component observation signals. This configuration provides high temporal resolution and low noise characteristics, thereby enabling stable capture of high-quality waveforms of microtremor signals in an urban environment, as indicated by the data.

The spatial distribution of the observation points ensures adequate coverage of the study area, thereby enabling reliable characterization of lateral site variability and providing a solid foundation for subsequent frequency domain analysis and inversion procedures.

3 Application Cases

3.1 Site Engineering Conditions

The study site is located in the Youjiang (Right River) District of Baise City, Guangxi Province, China. The investigated structure is a 33 story reinforced concrete civil complex with a total height of 99 m. The site lies on the first terrace of the Youjiang River, with a ground elevation of approximately 125 m above sea level. Prior to construction, detailed borehole investigations were conducted in the surrounding area to characterize the subsurface geological conditions. The borehole data indicate that the stratigraphic sequence comprises vegetal fill, alluvial clay, silty clay, pebble layers, and underlying Tertiary mudstone, reflecting a typical alluvial depositional environment.

As shown in Table 1, the characteristic period of the design response spectrum in the study area (Youjiang District, Baise City, Guangxi, China) is approximately 0.35 s, the peak ground acceleration is approximately 0.10 g, and a damping ratio of 5% is adopted. The study area is located in the South China block, which is characterized by relatively low-to-moderate seismic activity. The adopted seismic parameters are consistent with the national seismic hazard zonation framework of mainland China and fall within typical ranges reported in previous probabilistic seismic hazard studies [27–29]. A damping ratio of 5% is adopted as standard engineering practice in seismic response analysis.

Table 1: Seismic design parameter zones and representative values.

Parameter	Zone Value	Zone Range	Study Site (Youjiang District, Baise City)
PGA (g)	0.05 g	$0.04 \le PGA < 0.09$	≈0.10 g
	0.10 g	$0.09 \le PGA < 0.14$	
	0.15 g	$0.14 \le PGA < 0.19$	
	0.20 g	$0.19 \le PGA < 0.28$	
	0.30 g	$0.28 \le PGA < 0.38$	
	0.40 g	$0.38 \le PGA < 0.75$	
Tg (s)	0.35 s	$Tg \le 0.40$ s	≈0.35 s
	0.40 s	$0.40 < Tg < 0.45$ s	
	0.45 s	$Tg \ge 0.45$ s	

Note: The values for the study site are approximate representative values within the corresponding zonation ranges.

3.2 Data Processing

Fig. 2 illustrates the H/V spectral ratio curves derived from three representative free-field measurement points within the study area, which were selected to enhance comparison and improve result interpretability. These points are distributed across different zones of the site, enabling an evaluation of the effects of overburden thickness, soil stiffness, and subsurface structural heterogeneity on the characteristics of the H/V spectral ratios. As shown in the figure, all measurement points exhibit distinct and well defined peaks, indicating clear site resonance behavior.

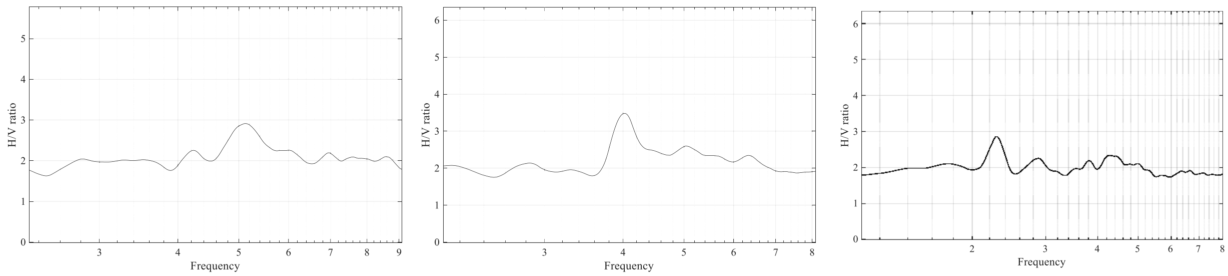

Figure 2: H/V spectral ratio curves for sites in the study area.

To clarify the shallow subsurface structure and improve geological interpretation of the study area, three component microtremor records were analyzed using the H/V spectral ratio method. Baseline correction and spectral smoothing were performed to enhance data quality and ensure reliable spectral estimates. The f_0 and amplification factor were extracted to characterize local site response. These parameters were spatially interpolated and mapped to illustrate lateral variations in site conditions and to provide quantitative insight into subsurface heterogeneity.

Fig. 3a shows that the f_0 values derived from 101 ambient vibration observation points in the study area range from 2.29 to 6.71 Hz. Pronounced spatial variability in f_0 is observed among different measurement points, reflecting the lateral heterogeneity of shallow geological structures and variations in overburden thickness. f_0 values between 2 and 5 Hz dominate the central and western parts of the study area, indicating relatively uniform shallow cover thickness and comparable dynamic properties of the near-surface materials. In contrast, f_0 values exceeding 6 Hz occur only in localized zones, which are primarily associated with thin surficial deposits or the presence of high-stiffness subsurface media.

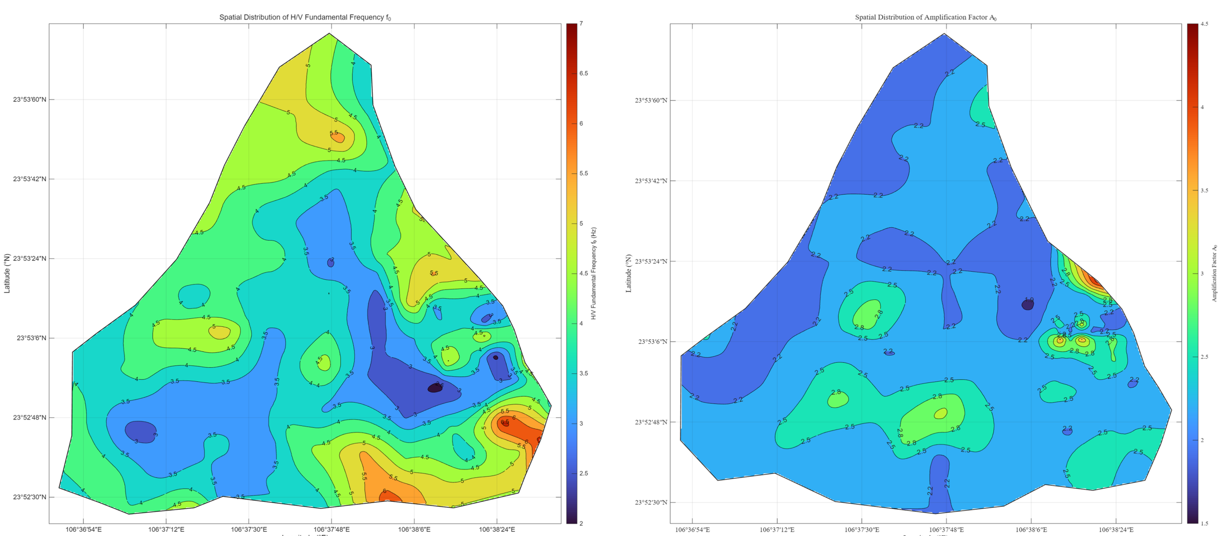

(a) **(b)**

Figure 3: (Continued)

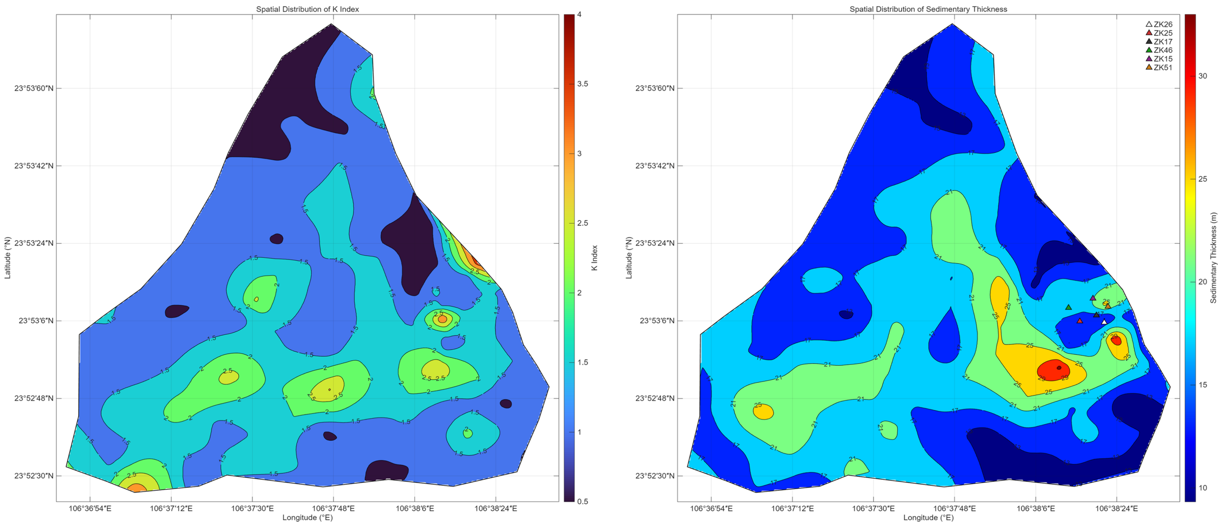

(c) (d)

Figure 3: Spatial distribution of site dynamic parameters in the study area. (**a**) Contour map of the H/V fundamental peak frequency derived from ambient vibration measurements; (**b**) spatial distribution of the site amplification factor A_0 obtained from H/V spectral ratios; (**c**) spatial distribution of the site vulnerability index K; (**d**) contour map of sedimentary layer thickness estimated from the H/V fundamental frequency.

According to Eq. (2), the site characteristic period in the study area ranges from 0.15–0.44 s. The overall distribution closely overlaps with the characteristic period of 0.35 s adopted in the design response spectrum. This correspondence indicates that shallow site dynamic characteristics derived from ambient vibration analysis are consistent with the site conditions assumed in engineering design. Such agreement provides a reliable basis for investigating the influence of site effects on the vibration response of high-rise buildings, particularly the amplification behavior observed in the floor response spectra.

By further calculating the A_0 and K indices for the study area and mapping their spatial distributions (Fig. 3b,c), the site dynamic response characteristics can be interpreted from multiple perspectives. As shown in Fig. 3b, the A_0 index primarily reflects the site's capacity to amplify ground motion, whereas the K index presented in Fig. 3c integrates both the fundamental frequency and amplification effects, thereby serving as a strong indicator of site dynamic vulnerability. These parameters are essential for identifying zones with potential strong amplification and for delineating site vulnerability within the study area. In addition, they provide a quantitative basis for subsequent inversion of the sedimentary layer structure and for analyzing site-structure coupled effects.

Fig. 3d presents the spatial distribution of h inverted from f_0 using the empirical relationship. The values generally range from approximately 10 m to over 30 m and exhibit pronounced lateral heterogeneity. Larger values are mainly concentrated in the central and southeastern parts of the study area, whereas smaller values occur in localized northeastern and marginal zones. The distribution shows a clear inverse correlation with the f_0 pattern in Fig. 3a, where lower f_0 values correspond to greater h. This spatial consistency supports the reliability of the ambient vibration–based inversion and enhances the interpretation of shallow subsurface structural characteristics.

By establishing a quantitative relationship between h and the H/V-derived f_0 in the study area, an empirical relationship was developed using data from six boreholes and E–N–Z ambient vibration measurements recorded at adjacent sites. Specifically, the relationship was obtained by fitting the H/V-derived f_0 to the corresponding h values from borehole data using a least-squares regression method. The resulting empirical model yields a coefficient of determination of R^2 = 0.9543, indicating a strong correlation and a high level of consistency between h and f_0.

$$h = 90.05 f_0^{-1.203} \tag{8}$$

To verify the applicability of the proposed empirical relationship, the H/V-derived f_0 obtained from ambient vibration measurements adjacent to boreholes were substituted into Eq. (8) to estimate h. The calculated values were compared with the soil-rock interface depths identified from borehole investigations, and the results are summarized in Table 2. The estimated h values show good agreement with measured values, with relative errors remaining within a limited range, demonstrating the reliability of the inversion.

Table 2: Drilling information and calculation errors.

Drill Hole	Drilling Depth (m)	Measuring Point	Frequency (Hz)	Fit Depth (m)	Relative Error (%)
ZK26	11.80	03	5.11	12.56	+6.44%
ZK25	15.80	01	4.02	16.89	+6.90%
ZK17	17.50	05	3.73	18.53	+5.89%
ZK46	19.10	21	3.51	19.93	+4.35%
ZK15	20.80	20	3.43	20.44	−1.73%
ZK51	24.30	06	2.81	25.36	+4.36%

Following validation, the proposed relationship was further compared with existing empirical formulas reported in previous studies, as summarized in Table 3. Although the functional form consistently follows a power-law decay, variations in empirical coefficients reflect regional geological conditions, sedimentary structures, and V_s characteristics.

Table 3: Comparison of empirical relationships between f_0 and sediment thickness and their applicable conditions.

Reference	Empirical Relationship	Study Area	Frequency (Hz)	Remarks
This study	$h = 90.05 f_0^{-1.203}$	Right River District, Baise, China; 106 sites, 6 boreholes	2.29–6.71	Sedimentary layer thickness ranges from 9 to 34 m
[30]	$h = 55.64 f_0^{-1.268}$	Bajo Segura Basin, Spain; 23 stations	1–10	Sedimentary thickness less than 100 m; shear wave velocity < 250 m/s
[31]	$h = 62.67 f_0^{-1.097}$	Nanning City, Guangxi, China; 561 points compared with 4 boreholes	1–10	Most thicknesses between 10 and 40 m
[32]	$h = 103.20 f_0^{-1.251}$	Sanhe–Pinggu area, China; 3 boreholes and 4 arrays	0.2–10	Shallow shear wave velocity < 180 m/s

(Continued)

Table 3 (continued)

Reference	Empirical Relationship	Study Area	Frequency (Hz)	Remarks
[33]	$h = 55.00 f_0^{-1.020}$	Pearl River Delta, China; 52 boreholes	1–10	Sedimentary thickness 7.9–39.6 m
[34]	$h = 90.00 f_0^{-1.388}$	Lower Rhine Embayment, Germany; 34	0.14–4.5	Cover thickness 30–1600 m; shear-wave velocity varies significantly

Fig. 4 provides a graphical illustration of these results. Fig. 4a presents the cross-sectional comparison between inverted and measured thicknesses, confirming the fitting accuracy. Fig. 4b compares empirical relationships derived from different regions, highlighting both the consistent functional trend and regional parameter differences.

To evaluate how site-controlled excitation influences structural response, acceleration monitoring was conducted at representative elevations of the 33-story building. The structural layout, sensor configuration, and recorded time histories are presented in Fig. 5. The recorded acceleration time histories exhibit a clear vertical variation in structural response amplitude. In the horizontal direction, the roof shows the largest acceleration, followed by the middle floor, while the foundation level exhibits comparatively small motion. This progressive amplification with height is consistent with the expected deformation characteristics of high-rise structures dominated by the fundamental vibration mode, in which lateral displacement increases from the constrained base toward the top.

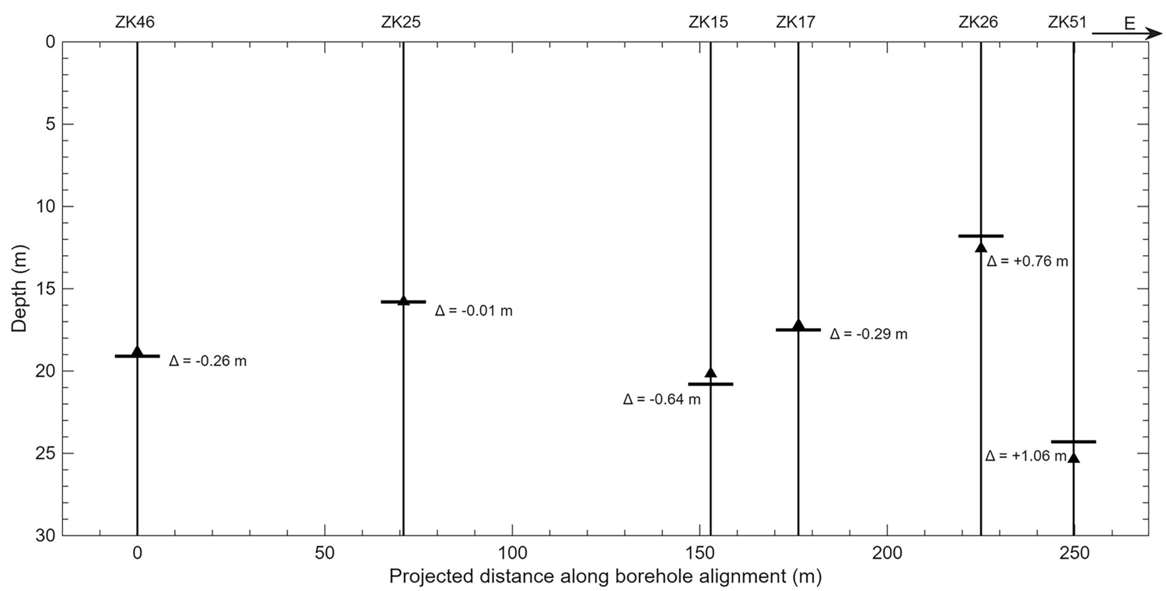

(a)

Figure 4: (Continued)

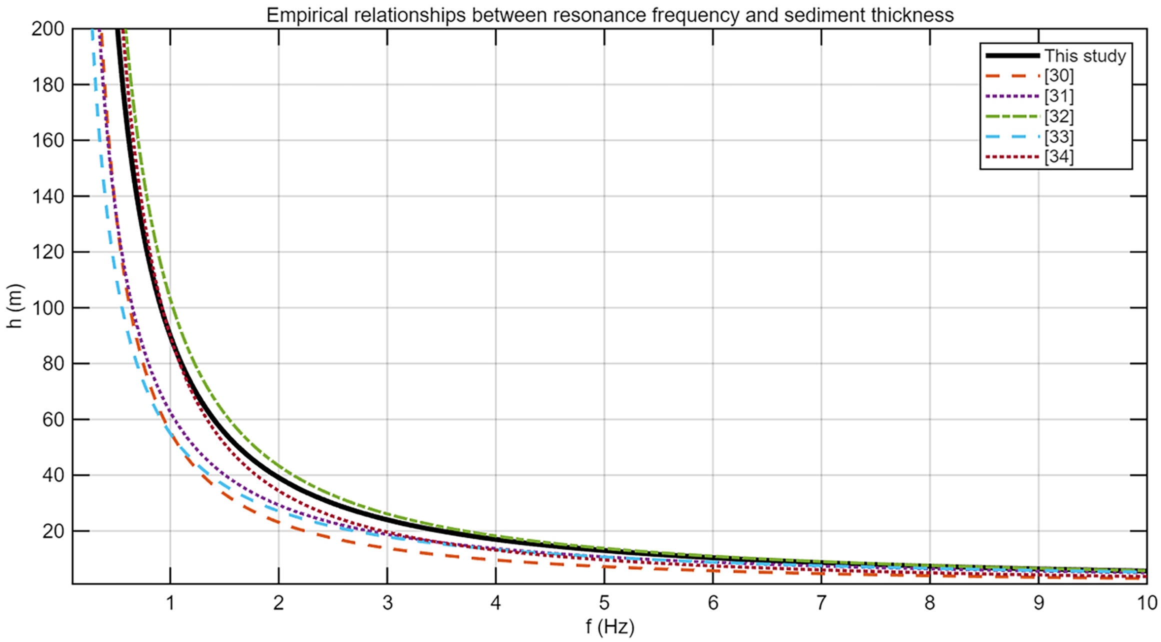

(b)

Figure 4: (**a**) Depth profile of soil-rock interface. ▲ represents the depth of the soil-rock interface calculated according to Formula (8), and the vertical line represents the borehole. The short horizontal line on the vertical line represents the depth of the soil-rock interface revealed by the borehole, and Δ represents the absolute error of the calculation; (**b**) empirical relationship between the thickness of the deposited layer at different regional resonance frequencies [30–34].

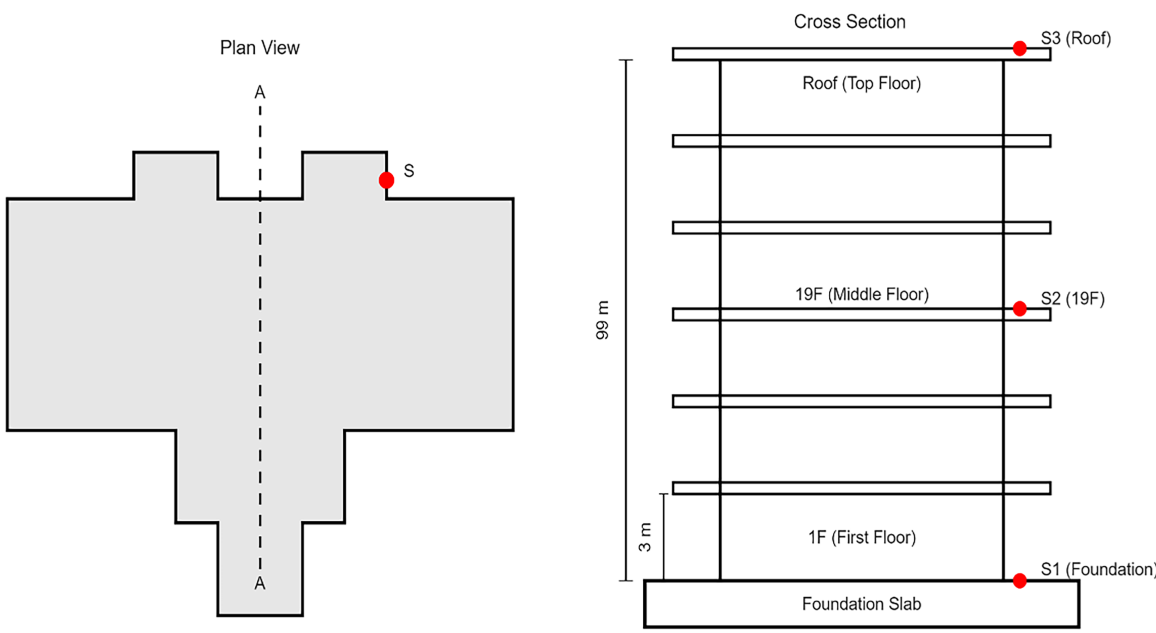

(a)

Figure 5: (Continued)

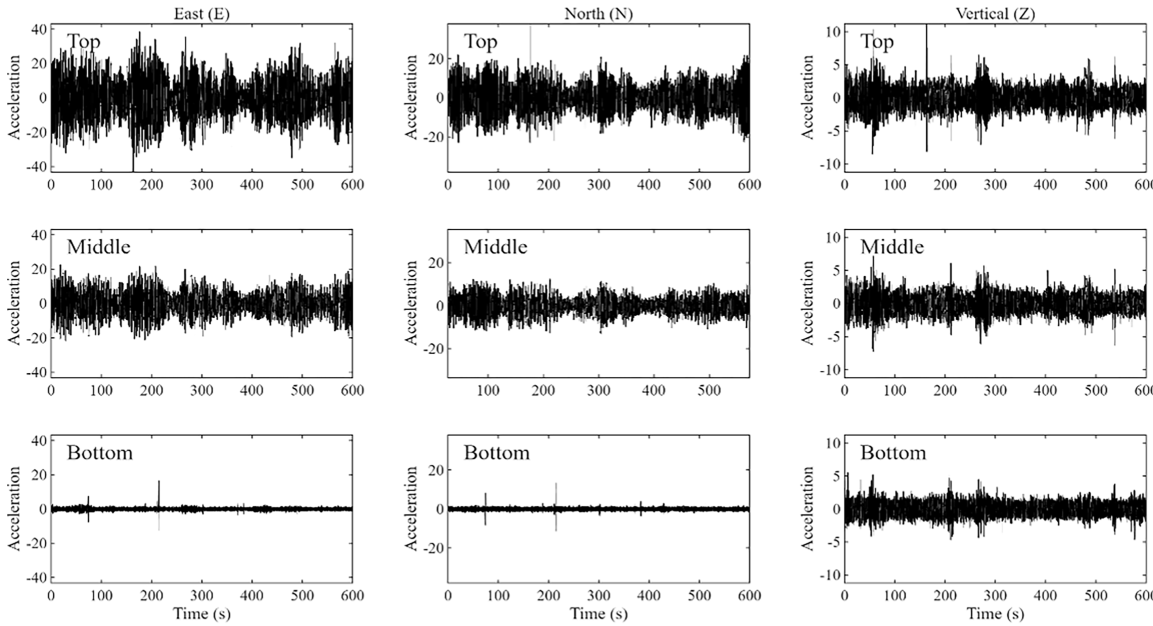

(b)

Figure 5: (**a**) Structural layout and sensor configuration of the 33-story building. The dashed line A–A denotes the section line, and S indicates the sensor position; (**b**) E–N–Z acceleration time histories recorded at the foundation, 19th floor, and roof.

Notably, the horizontal components at the foundation level remain significantly smaller than those at the upper floors. This phenomenon reflects the strong boundary constraint and high stiffness near the structural base. Under dominant first-mode participation, lateral displacement and corresponding acceleration are inherently limited close to the fixed base, resulting in reduced E and N responses at the foundation. In contrast, the vertical component remains relatively comparable across different elevations, indicating more direct transmission of ground vibration through the load-bearing system. These observations collectively highlight the modal-controlled redistribution of structural acceleration along the building height.

Although the time histories reveal clear height-dependent amplification, time-domain observations alone cannot fully characterize the frequency-dependent behavior of structural response. To further examine how foundation excitation is redistributed along the building height, the superstructure response was analyzed using floor response spectra. By comparing spectral amplification between different floor levels, the combined influence of site-controlled input and structural modal characteristics on the vertical distribution of seismic response can be identified. The resulting horizontal and vertical spectral amplification factors are presented in Fig. 6.

The dynamic behavior of the investigated 33-story reinforced concrete building was examined using ambient vibration measurements recorded at three representative levels: the bottom floor (1F), a mid-height floor (19F), and the roof level (33F). Fourier spectra of the microtremor records were first computed for both vertical and horizontal components. To identify the modal characteristics of the structure, three floor Fourier spectral ratios were evaluated, namely Top/Bottom, Mid/Bottom, and Top/Mid, defined as follows:

$$S(f) = \frac{S_{upper}(f)}{S_{lower}(f)}, \tag{9}$$

where $S(f)$ denotes the spectral ratio at frequency f, and $S_{upper}(f)$ and $S_{lower}(f)$ represent the Fourier amplitude spectra recorded at the upper and lower floors, respectively. These ratios provide a convenient way to visualize the relative amplification of vibration along the height of the building and to infer the associated modal deformation patterns.

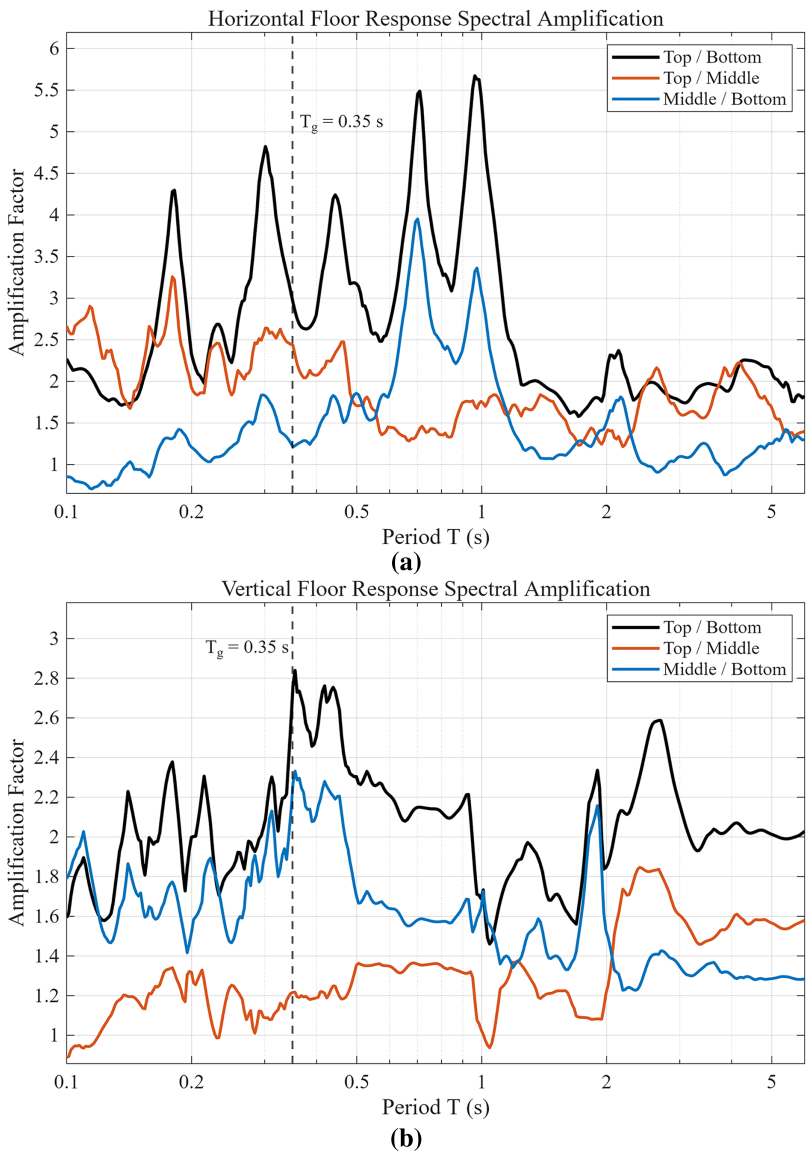

Figure 6: Characterization of floor response spectra between different floors. (**a**) Horizontal floor response spectral amplification; (**b**) vertical floor response spectral amplification.

The horizontal spectral ratios reveal several distinct peaks at approximately 0.45, 0.70, and 1.00 s, as illustrated in Fig. 6a, indicating the presence of multiple vibration modes in the lateral direction. Among these, the peak near T ≈ 0.70 s is interpreted as the fundamental global bending mode of the structure. This interpretation is supported by the moderate Top/Mid ratio (approximately 1.5), which indicates that the vibration amplitude increases smoothly with height, a characteristic feature of first-mode bending deformation in high-rise buildings. The shorter period near T ≈ 0.45 s exhibits a significantly larger Top/Mid ratio (approximately 2.5), suggesting stronger amplification in the upper portion of the building. This behavior is consistent with vibration in the stiffer horizontal direction of a rectangular-plan structure, where the shorter structural dimension leads to a smaller fundamental period. Meanwhile, the longer period near T ≈ 1.00 s, where the Top/Mid ratio increases again to about 1.8, likely corresponds to a higher-order bending mode or a coupled vibration mode involving more complex deformation patterns.

For the vertical component, the spectral ratios exhibit a clear dominant peak at approximately T ≈ 0.36 s, as shown in Fig. 6b, indicating the presence of a primary axial vibration mode governed mainly by the vertical stiffness of the structural system. The amplification pattern generally follows the hierarchy Top/Bottom > Mid/Bottom > Top/Mid, suggesting that the vertical vibration amplitude increases gradually from the base to the roof. Such behavior is consistent with the deformation pattern expected in a vertically continuous structural system subjected to base excitation. In addition, the three spectral ratios approximately satisfy the relationship Top/Bottom ≈ Mid/Bottom × Top/Mid, which reflects the internal consistency among the measured spectral ratios and confirms that the observed amplification pattern along the building height is controlled by a continuous modal deformation rather than by localized structural anomalies. Furthermore, no significant vertical amplification is observed near the dominant horizontal modal periods, suggesting that vertical and horizontal structural responses are largely decoupled.

An additional feature is observed in the horizontal component at shorter periods (T < 0.5 s), where the amplification hierarchy becomes Top/Bottom > Top/Mid > Mid/Bottom, as also observed in Fig. 6a. This pattern indicates that the mid-height level exhibits relatively smaller vibration amplitudes compared with the roof level. Such behavior can be attributed to higher-order bending modes, in which nodal regions may occur near intermediate levels, thereby reducing the response amplitude at those levels. The relatively smooth amplification patterns observed in both vertical and horizontal components further suggest that the structural stiffness distribution along the building height is reasonably continuous, with no pronounced structural irregularities such as soft-story effects or abrupt stiffness discontinuities.

Although the shortest structural period (T ≈ 0.45 s) is close to the upper bound of the site characteristic period range (0.15–0.44 s), no distinct resonance-type amplification is identified in the floor response spectra. This clearly indicates that the observed amplification behavior is not governed by classical site–structure resonance, but is instead controlled by the combined effects of site-induced spectral modulation and the intrinsic modal characteristics of the structure under frequency mismatch conditions.

4 Discussion

The ambient vibration analysis provides important insight into the dynamic characteristics of the shallow subsurface conditions in the study area. The H/V spectral ratio results indicate that f_0 ranges from approximately 2.29 to 6.71 Hz, corresponding to characteristic site periods between about 0.15 and 0.44 s. This range is generally consistent with the characteristic period of 0.35 s specified in the regional seismic design spectrum. In addition, the sediment thickness inverted from the H/V dominant frequencies varies from approximately 10 m to over 30 m across the study area, indicating pronounced lateral heterogeneity in shallow geological conditions. Such variability in sediment thickness influences the resonance characteristics of the site and therefore affects the frequency content of the ground motion transmitted to the building foundation.

The structural response analysis further reveals distinct dynamic characteristics of the investigated high-rise building. The floor response spectral ratios indicate that the dominant vertical vibration occurs at approximately 0.36 s, while the horizontal response exhibits several peaks near 0.45, 0.70, and 1.00 s, corresponding to different vibration modes of the structure. Among these, the peak around 0.70 s represents the fundamental bending mode governing the lateral response. The gradual increase of spectral amplification toward the upper levels reflects the typical deformation pattern of high-rise structures dominated by bending behavior, while the relatively smooth amplification distribution along the building height indicates a continuous stiffness profile without pronounced soft-story effects.

When compared with the site characteristic period range (0.15–0.44 s), none of the identified structural periods strictly coincide with the dominant site frequencies. Although the shortest structural period (T ≈ 0.45 s) is close to the upper bound of the site period range, no distinct resonance-type amplification is observed in the floor response spectra. The fundamental structural period (T ≈ 0.70 s) and higher-order modes (T ≈ 1.00 s) are clearly separated from the site-controlled frequency band. These observations demonstrate that the structural response is not governed by classical site–structure resonance, but rather by a coupling mechanism in which the site modifies the spectral characteristics of the input motion, while the structure selectively amplifies specific frequency components according to its modal properties, reflecting a frequency-mismatch-controlled interaction governed by spectral modulation and modal filtering.

It should be noted that the interpretation of H/V results in this study is subject to certain limitations. The method is primarily based on the assumption of horizontally layered media and may not fully capture complex subsurface conditions in urban environments. In particular, lateral heterogeneity, basin effects, and three-dimensional geological structures may contribute to the observed spectral characteristics. Therefore, the identified f_0 and inferred sediment thicknesses should be interpreted as effective parameters reflecting the dominant site response, rather than unique solutions of the subsurface structure. The incorporation of borehole data in this study partially reduces this limitation by providing independent constraints. Future work should integrate additional passive or active seismic methods, such as surface-wave dispersion analysis or array-based techniques, to further improve the reliability of subsurface characterization.

Uncertainty is an inherent aspect of subsurface parameter estimation based on ambient vibration data. In this study, several sources of uncertainty should be considered. A sensitivity analysis shows that a perturbation of ±0.1 Hz in f_0 propagates to a thickness uncertainty of ±0.30–1.11 m (±2.4%–4.3%), and a perturbation of ±0.2 Hz results in ±4.7%–8.6%, across the range of measured frequencies (2.81–5.11 Hz). The relative errors reported in Table 2 (ranging from −1.73% to +6.90%) are of comparable magnitude to this sensitivity range, suggesting that f_0 estimation uncertainty is a plausible contributing factor to the observed inversion discrepancies, alongside regional geological variability. Second, the empirical relationship used for sediment thickness inversion introduces uncertainty due to regional geological variability. Third, spatial heterogeneity of shallow sediments may lead to deviations from simplified assumptions. Despite these uncertainties, the comparison between inverted results and borehole data demonstrates relatively small discrepancies, indicating that the proposed approach provides a reasonable approximation of shallow subsurface conditions for engineering applications. Previous studies have highlighted the importance of probabilistic approaches in shear-wave velocity modeling [35]. In principle, V_s can be inferred from the relationship between f_0 and thickness based on the quarter-wavelength theory. However, this inversion is inherently non-unique and sensitive to uncertainties in f_0 estimation and subsurface heterogeneity.

5 Conclusions

This study investigates the coupling between shallow site conditions and the dynamic response of a high-rise building using ambient vibration observations. By integrating site characterization and structural response analysis, the main findings can be summarized as follows:

(1) The H/V spectral ratio analysis reveals pronounced spatial heterogeneity in the shallow sedimentary structure within the study area. The f_0 ranges from approximately 2.29 to 6.71 Hz, corresponding to 0.15–0.44 s, which are generally consistent with the design value of 0.35 s specified in the regional seismic zoning map. Based on the empirical relationship established using ambient vibration measurements and borehole data, the inverted h ranges from approximately 10 m to over 30 m, indicating

significant lateral variability of shallow subsurface conditions. A clear negative correlation between f_0 and h is observed, providing a reliable basis for estimating shallow subsurface structure using ambient vibration data.

(2) Floor response spectral ratio analysis reveals distinct modal characteristics of the investigated high-rise structure. The vertical component exhibits a dominant peak at approximately T ≈ 0.36 s, while the horizontal spectral ratios display several peaks near 0.45, 0.70, and 1.00 s, with the peak around 0.70 s corresponding to the fundamental global bending mode governing the lateral response of the building. The gradual increase of spectral amplification toward the upper floors reflects the typical deformation pattern of high-rise structures dominated by bending behavior, providing insight into the height-dependent amplification characteristics of structural response.

(3) The comparison between site characteristics and structural dynamic properties shows that no clear resonance-type amplification occurs, despite the partial overlap between 0.15–0.44 and 0.45 s. The structural response is governed by a frequency-mismatch mechanism, in which the input motion is spectrally modified by the site, while the structure selectively amplifies specific frequency components according to its modal properties. This finding highlights that structural response is controlled by spectral modulation and modal filtering rather than classical resonance, providing a new perspective for evaluating site–structure interaction in high-rise buildings.

Overall, this study provides a practical framework for understanding site–structure interaction under frequency-mismatch conditions, offering valuable implications for seismic response assessment and performance-based design of high-rise buildings.

Acknowledgement: Not applicable.

Funding Statement: The authors received no specific funding for this study.

Author Contributions: Yangkai Ou contributed to conceptualization, methodology, data collection, formal analysis, visualization, and writing—original draft preparation. Boi-Yee Liao contributed to supervision, validation, and writing—review and editing. All authors reviewed and approved the final version of the manuscript.

Availability of Data and Materials: The data that support the findings of this study are available from the corresponding author (Boi-Yee Liao) upon reasonable request.

Ethics Approval: Not applicable.

Conflict of Interest: The authors declare no conflicts of interest.

References

1. Araz O, Ozturk KF, Cakir T. Effect of soil-structure interaction on story acceleration response of a high-rise building. Soil Mech Found Eng. 2024;61(1):42–8. doi:10.1007/s11204-024-09941-3.
2. Srivastava M, Sharma ML. Site characterization of southern Bihar region employing topographic slope as a proxy: implication to seismic scenario. J Earth Syst Sci. 2025;134(2):116. doi:10.1007/s12040-025-02578-2.
3. Tian Y, Chen S, Liu S, Lu X. Influence of tall buildings on city-scale seismic response analysis: a case study of Shanghai CBD. Soil Dyn Earthq Eng. 2023;173(1):108063. doi:10.1016/j.soildyn.2023.108063.
4. Zhang X, Far H. Effects of dynamic soil-structure interaction on seismic behaviour of high-rise buildings. Bull Earthq Eng. 2022;20(7):3443–67. doi:10.1007/s10518-021-01176-z.
5. Kang SY. Mapping bedrock topography and detecting blind faults using the fundamental resonance of microtremor: a case study of the Pohang Basin, southeastern Korea. Geophys J Int. 2024;238(2):806–19. doi:10.1093/gji/ggae194.

6. Putti SP, Satyam N. Evaluation of site effects using HVSR microtremor measurements in Vishakhapatnam (India). Earth Syst Environ. 2020;4(2):439–54. doi:10.1007/s41748-020-00158-6.
7. Antonovskaya GN, Danilov KB, Basakina IM, Afonin NY, Kapustian NK. Application examples and capabilities of combining passive seismic methods to study depth structure of the Earth's crust. Izv Phys Solid Earth. 2024;60(4):712–25. doi:10.1134/S1069351324700721.
8. Han Y, Zhao YG, Zhang H. Study on the microtremor horizontal-to-vertical spectral ratio based on response spectra. Bull Seismol Soc Am. 2025;115(5):2407–20. doi:10.1785/0120250019.
9. Kalinina AV, Ammosov SM, Tatevossian RE, Bykova VV. Applicability of the H/V method in the seismic microzoning problem. Seism Instrum. 2022;58(1):S79–88. doi:10.3103/S0747923922070052.
10. Xu R, Wang L. The horizontal-to-vertical spectral ratio and its applications. EURASIP J Adv Signal Process. 2021;2021(1):75. doi:10.1186/s13634-021-00765-z.
11. Zhang Y, Wei X, Li YE, Jeong S, Ku T. Sediment thickness and average vs. prediction using HVSR of ambient seismic noise: case studies in Singapore. Bull Eng Geol Environ. 2023;82(5):195. doi:10.1007/s10064-023-03195-3.
12. Chen S, Liu Q, Zhai C, Wen W. Influence of building-site resonance and building properties on site-city interaction: a numerical investigation. Soil Dyn Earthq Eng. 2022;158:107307. doi:10.1016/j.soildyn.2022.107307.
13. Ghione F, Köhler A, Dichiarante AM, Aarnes I, Oye V. Vs30 and depth to bedrock estimates from integrating HVSR measurements and geology-slope approach in the Oslo area. Norway Front Earth Sci. 2023;11:1242679. doi:10.3389/feart.2023.1242679.
14. Grassi S, Barbano MS, Pirrotta C, Morreale G, Imposa S. Seismic soil-structure interaction of three historical buildings at the university of Catania (Sicily, Italy). Heritage. 2022;5(4):3562–87. doi:10.3390/heritage5040185.
15. Yao J, Wu Z, Cao X, Wu N, Zhang N. Derivation and application of analytical coupling loss coefficient by transfer function in soil-building vibration. Buildings. 2024;14(7):1933. doi:10.3390/buildings14071933.
16. Haghshenas E, Bard PY, Theodulidis N, Team SW. Empirical evaluation of microtremor H/V spectral ratio. Bull Earthq Eng. 2008;6(1):75–108. doi:10.1007/s10518-007-9058-x.
17. Zhou Y, Zhou Y, Yi W, Chen T, Tan D, Mi S. Operational modal analysis and rational finite-element model selection for ten high-rise buildings based on on-site ambient vibration measurements. J Perform Constr Facil. 2017;31(5):04017043. doi:10.1061/(asce)cf.1943-5509.0001019.
18. Teves-Costa P, Matias L, Bard PY. Seismic behaviour estimation of thin alluvium layers using microtremor recordings. Soil Dyn Earthq Eng. 1996;15(3):201–9. doi:10.1016/0267-7261(95)00038-0.
19. Nakamura Y. A method for dynamic characteristics estimation of subsurface using microtremor on the ground surface. Railw Tech Res Inst Q Rep. 1989;30(1):25–33.
20. Bahri AS, Utama W, Aini DN, Lutfie MN. Valuation of building strength against earthquake vibrations using microtremor analysis (case study: the city of Surabaya). IOP Conf Ser Earth Environ Sci. 2016;29(1):012018. doi:10.1088/1755-1315/29/1/012018.
21. Gao W, Wang T, Dai J, Jin B. Study on floor-response spectrum of nuclear power plants considering soil-structure interactions. Eng Mech. 2020;37(10):116–24. doi:10.6052/j.issn.1000-4750.2019.11.0675.
22. Molnar S, Sirohey A, Assaf J, Bard PY, Castellaro S, Cornou C, et al. A review of the microtremor horizontal-to-vertical spectral ratio (MHVSR) method. J Seismol. 2022;26(4):653–85. doi:10.1007/s10950-021-10062-9.
23. Zhang R, Xu P, Ling S, Du Y, You Z, Wang Z, et al. Detection of the soil-rock interface based on microtremor H/V spectral ratio method: a case study of the Jinan urban area. Chin J Geophys. 2020;63(1):339–50. (In Chinese). doi:10.6038/cjg2020M0678.
24. Qin T, Wang S, Feng X, Lu L. A review on microtremor H/V spectral ratio method. Rev Geophys Planet Phys. 2021;52(6):587. doi:10.19975/j.dqyxx.2021-003.
25. Mokhberi M. Vulnerability evaluation of the urban area using the H/V spectral ratio of microtremors. Int J Disaster Risk Reduct. 2015;13(1):369–74. doi:10.1016/j.ijdrr.2015.06.012.
26. Gremer N, Adam C. Vertical floor acceleration spectra for regular steel frame structures. Structures. 2023;55(2):690–700. doi:10.1016/j.istruc.2023.06.051.
27. Li J, Wang Y, Chen H, Lin L. Risk assessment study of fire following an earthquake: a case study of petrochemical enterprises in China. Nat Hazards Earth Syst Sci. 2014;14(4):891–900. doi:10.5194/nhess-14-891-2014.

28. Rong Y, Xu X, Cheng J, Chen G, Magistrale H, Shen ZK. A probabilistic seismic hazard model for Mainland China. Earthq Spectra. 2020;36(1S):181–209. doi:10.1177/8755293020910754.
29. Ji K, Wen R, Ren Y, Wang W, Chen L. Disaggregation of probabilistic seismic hazard and construction of conditional spectrum for China. Bull Earthq Eng. 2021;19(14):5769–89. doi:10.1007/s10518-021-01200-2.
30. Delgado J, López Casado C, Giner J, Estévez A, Cuenca A, Molina S. Microtremors as a geophysical exploration tool: applications and limitations. Pure Appl Geophys. 2000;157(9):1445–62. doi:10.1007/PL00001128.
31. Ma H, Liao BY. Study on site effect in Nanning City using HVSR method. Cea. 2024;12(2):1165–79. doi:10.13189/cea.2024.120235.
32. Peng F, Wang W, Kou H. H/V spectral analysis of ground vibration in the Sanhe-Pinggu area: plateau response, shallow sedimentary structure and its reflected fault activity. Chin J Geophys. 2020;63(10):16. (In Chinese).
33. Liang D, Gan F, Zhang W, Jia L. The application of HVSR method in detecting sediment thickness in karst collapse area of Pearl River Delta, China. Environ Earth Sci. 2018;77(6):259. doi:10.1007/s12665-018-7439-x.
34. Ibs-von Seht M, Wohlenberg J. Microtremor measurements used to map thickness of soft sediments. Bull Seismol Soc Am. 1999;89(1):250–9. doi:10.1785/bssa0890010250.
35. Totani F, Aloisio A. Probabilistic shear wave velocity model based on downhole test database for Apennine flysch formations. Soil Dyn Earthq Eng. 2023;173(4):108132. doi:10.1016/j.soildyn.2023.108132.